On Half-Power Beamwidth of Intelligent Reflecting Surface

Han Han, Yihong Liu, *Graduate Student Member, IEEE*, and Lei Zhang, *Senior Member, IEEE*

***Abstract*—Half-power beamwidth (HPBW) is a key parameter to measure the performance of antenna array and the newly proposed intelligent reflecting surface (IRS) systems. In this paper, we first establish a system model for IRS in uniform linear array (ULA) and uniform rectangular array (URA) configurations, then the IRS HPBW in both cases are derived under the far-field condition without considering channel path-loss and fading. We find that in ULA and URA configurations, IRS HPBW is equal to antenna array's HPBW at the same reflect/transmit angle with maximal ratio combining applied, while IRS HPBW is always greater than or equal to antenna array's HPBW when all weights are equal. Besides, under certain incident angles, there will be abrupt changes in HPBW and the analytical expressions of the boundary values in both ULA and URA cases are provided. Unlike the traditional active antenna array, our conclusion shows that the IRS HPBW will change with the incident angles. Simulation results verify the correctness of our derivations.**

***Index Terms*—Antenna array, beamforming, half-power beamwidth, intelligent reflecting surface, reconfigurable intelligent surface.**

I. Introduction

THERE are many factors can limit the performance of wireless communication systems, among which the wireless channel is the most critical, intractable but indispensable one, since it is uncontrollable and unpredictable. Under the wireless propagation condition, the signal carried by electromagnetic (EM) wave is inevitably suffered from many channel effects such as path-loss and fading. To compensate the path-loss in the increasing distance between the receiver and transmitter, receiver sensitivity and/or transmission power can be increased but at a cost of increasing the system complexity and/or reducing power efficiency. Besides, to overcome the multi-path effect, algorithms and modulation schemes such as orthogonal frequency-division multiplexing (OFDM) were developed [1]. However, complex algorithms and systems also bring significant cost and power efficiency problems.

It would be no doubt that what a significant revolution of wireless communication can achieve if the channel can be controlled directly. Thanks to the development of EM materials in recent years, a new low-cost material [2] has been discovered, which is often referred to as meta-material [3]. On this basis, an artificial thin film, commonly known as the intelligent reflecting surface (IRS) (also known as RIS: Reconfigurable Intelligent Surface [4]) was developed. IRS acts as an EM mirror that can reflect signals transmitted from transmitter (Tx) to receiver (Rx) through optimized weights. To achieve this, IRS adjusts the weighting coefficient of each element on the surface, thus manipulates the phase and amplitude of the signal impinging on the IRS and reflect it to any desired direction. Based on this property, IRS is particularly useful in millimeter wave (mmWave) and Terahertz (THz) communications due to their severe coverage issues [5].

Different from the traditional active antenna array, IRS passively reflects impinging signals as an object rather than re-transmits the received signal as a transmitter. Because of its passive nature, IRS could be made as thin as a sheet of paper attaching on any surfaces and therefore it is flexible, low cost, and low power. Due to its advantages, extensive research has been done in terms of system design, channel estimation, and optimization, etc. Multiple-input-multiple-output (MIMO) model of IRS has been proposed and analyzed by using minimal mean-squared error and zero-forcing beamforming [6]. In IRS-enhanced wireless communication system, some channel estimation and reflection optimization methods based on IRS-aided OFDM [7], [8] have been proposed. In addition, the existing experimental results [9] mostly focus on the pathloss modeling in IRS system.

As aforementioned, most of the existing works focus on the beamforming weights optimization for IRS. However, to the best of authors' knowledge, the key parameters of IRS are less focused, such as half-power beamwidth (HPBW), power gain, radiation pattern, and receiving antenna aperture, which are the foundation of many algorithms and practical systems. Among all the basic parameters, HPBW is no doubt one of the most important measurements of the directional radiation performance of the beamforming. For most of the cases, when the HPBW of every single piece of IRS is determined can an IRS-based communication network be taken into real engineering applications, especially for mmWave or THz communications. In IRS assisted robust beamforming, direction of arrival (DoA)/channel estimation, and link budget calculation, the IRS HPBW as a guideline is critically important. Besides, the establishment of HPBW also provides a basis for the further development of IRS algorithms. For instance, many algorithms focus on finding the best reflection direction of each beam to achieve the optimized channel allocation, it is critical to specify the performance of the IRS with reflection angles at these directions, while HPBW is the valid metric to measure the performance. Thus, a well-considered and thorough analysis of HPBW is required and an analytical expression of HPBW can guide the design, algorithms, and practical system deployment of the IRS.

In this paper, our study focuses on the expressions of HPBW on two commonly used IRS configuration, uniform linear array (ULA) and uniform rectangular array (URA). To summarize, the main contributions of this paper are as follows.

H. Han is with the Glasgow College, University of Electronic Science and Technology of China, Chengdu 611731, China (e-mail: 2357685h@student.gla.ac.uk).

Y. Liu and L. Zhang (corresponding author) are with James Watt School of Engineering, University of Glasgow, Glasgow G12 8QQ, U.K. (e-mail: y.liu.6@research.gla.ac.uk; lei.zhang@glasgow.ac.uk)

- Referring to the beamforming and signal transmission process, we first establish the channel model for IRS in both ULA and URA configurations by using antenna array theory. The array factor and steering vectors for the IRS are derived accordingly.
- Based on the proposed model and existing HPBW derivation of tradition active antenna array [10], the analytical expressions of IRS HPBW for both ULA and URA configurations are derived. By comparison, we find that the HPBW of IRS will change with incident angles. In ULA and URA configurations, IRS HPBW is equal to antenna array's HPBW at the same reflect/transmit angle with maximal ratio combining (MRC) applied, while IRS HPBW is always greater than or equal to antenna array's HPBW when all weights are equal.
- We find that when the incident angles reach into some specific regions, there will be some abrupt changes in the HPBW. By analyzing, we give the analytical expressions of the boundary values for both ULA and URA cases.

In this paper, bold-faced letters and lightfaced letters are used to denote column vectors and scalar quantities, respectively. Superscripts $(\cdot)^T$ and $(\cdot)^H$ represent the vector transpose and conjugate transpose, respectively. $\odot$ denotes the point-wise multiplication. We use the notations shown in Table I to describe our model and results.

TABLE I: Notations

Symbol	Definition
θ_{in}	Incident elevation angle
θ_{out}	Elevation angle of reflection
ψ_{in}	Incident azimuth angle
ψ_{out}	Azimuth angle of reflection
λ	Wavelength
k	Wave number, where $k = \frac{2\pi}{\lambda}$
M	Number of array elements
d	Elements spacing in ULA
Θ	Half-power beamwidth
a,b,c	Boundary value for ULA and URA
$(\cdot)_x$	Indicates physical quantities on X-axis
$(\cdot)_y$	Indicates physical quantities on Y-axis
$(\cdot)_h$	Indicates physical quantities at half-power decay point
$(\cdot)_e$	Indicates physical quantities on elevation plane in URA IRS
$(\cdot)_t$	Indicates physical quantities in tradition active antenna array
$(\cdot)_{MRC}$	Indicates physical quantities under MRC algorithm

II. System Model

IRS takes the role of steering the impinging signals to the desired direction by automatically adjusting the weights to control the whole channel. Since IRS is actually an EM reflection surface, we build a system model to describe the signal transmission process of IRS.

Though the shape of IRS could be arbitrary in theory, we consider two most commonly used configurations, i.e., ULA and URA and make them become the cornerstone for further study. We also assume far-field transmission, without considering channel path-loss and fading. In our model, line of sight (LoS) paths are considered between the Tx to IRS and IRS to Rx. There is no direct link between Tx and Rx. This assumption could be justified since IRS becomes more important in the case of no LoS path that exists between Tx and Rx, which could be an imperative issue in high-frequency bands (e.g., mmWave) communications.

A. IRS Model

Consider an IRS with M elements which is deployed for one pair of single antenna user communication. Assume $\boldsymbol{a}(\boldsymbol{\Omega}_{in})$ is the channel vector (steering vector) from Tx to the IRS and can be represented as

$$\boldsymbol{a}(\boldsymbol{\Omega}_{in}) = [a(\boldsymbol{\Omega}_{in,1}), \cdots, a(\boldsymbol{\Omega}_{in,M})]^T \in \mathbb{C}^{M\times 1} \ , \quad (1)$$

where $a(\boldsymbol{\Omega}_{in,m})$ is the phase quantity of incident direction and $\boldsymbol{\Omega}_{in,m}$ is the term containing the spatial information of incident direction from Tx at m-th element. In detail, $\boldsymbol{\Omega}$ is a function of azimuth and elevation angles for two-dimensional deployment (e.g. URA), or only contains one-dimensional information of azimuth angle such as ULA.

At Rx, the received signal reflected from the IRS are phased by another steering vector $\boldsymbol{a}(\boldsymbol{\Omega}_{out})$ and it could be defined as

$$\boldsymbol{a}(\boldsymbol{\Omega}_{out}) = [a(\boldsymbol{\Omega}_{out,1}), \cdots, a(\boldsymbol{\Omega}_{out,M})]^T \in \mathbb{C}^{M\times 1} \ , \quad (2)$$

where $\boldsymbol{\Omega}_{out,m}$ is the term containing the spatial information of reflected direction from IRS to Rx at m-th element. Since the incident and reflection steering vectors are independent to each other, we could then define a compound steering vector $\boldsymbol{a}_C(\boldsymbol{\Omega}_{in}, \boldsymbol{\Omega}_{out})$ which is merged by $\boldsymbol{a}(\boldsymbol{\Omega}_{in})$ and $\boldsymbol{a}(\boldsymbol{\Omega}_{out})$ that

$$\boldsymbol{a}_C(\boldsymbol{\Omega}_{in}, \boldsymbol{\Omega}_{out}) = \boldsymbol{a}(\boldsymbol{\Omega}_{in}) \odot \boldsymbol{a}(\boldsymbol{\Omega}_{out}) \ . \quad (3)$$

By referring to existing model [11], the equivalent channel $\widetilde{H}$ from Tx to Rx by considering IRS weights can be written as

$$\widetilde{H} = \boldsymbol{w}^H \cdot \boldsymbol{a}_C(\boldsymbol{\Omega}_{in}, \boldsymbol{\Omega}_{out}) \ , \quad (4)$$

where $\boldsymbol{w}$ is the weights vector with each entity being the weight of each surface element.

It is in common assumption to omit $\boldsymbol{w}$ (e.g., all elements are equal to 1) in (4) for beampattern and HPBW calculation due to the following reasons. For an Rx at a given location, no matter where the Tx is, we can always find an optimal solution by using MRC algorithm [12], so that the beampattern and HPBW under incident signals from different directions are the same. In a special case that the Tx, Rx are mirror-distributed with respect to IRS, the optimal $\boldsymbol{w}$ is a unit one vector by using MRC ($\boldsymbol{w}$ can be omitted). In this case, the array factor (AF) of IRS is a function of $\boldsymbol{\Omega}$ and can be expressed as

$$AF = \boldsymbol{a}^T(\boldsymbol{\Omega}_{out}) \cdot \boldsymbol{a}(\boldsymbol{\Omega}_{in}) \ . \quad (5)$$

Since the normalized AF is the mathematical representation of the beampattern, we can find that the beampattern and HPBW will change with the incident angles according to (5).

B. Steering Vector

Due to the different IRS coordinate systems in ULA and URA configurations, the incidence angle range of the two different configurations is different. In ULA IRS, $\theta_{in} \in (0, \pi)$ and $\psi_{in} \in (0, \pi)$; In URA IRS, $\theta_{in} \in (0, \frac{\pi}{2})$ and $\psi_{in} \in (0, 2\pi)$. Considering an IRS with M elements distributed uniformly in a line of ULA that is deployed for one pair of single-antenna users communication, we choose elevation angle θ for derivation (i.e., $\boldsymbol{\Omega}_{in} = \theta_{in}$, $\boldsymbol{\Omega}_{out} = \theta_{out}$). In this case, the steering vector for ULA could be expressed as

$$\begin{aligned}\boldsymbol{a}_C(\boldsymbol{\Omega}_{in}, \boldsymbol{\Omega}_{out}) = [1, & e^{jkd(\cos\theta_{in}+\cos\theta_{out})}, e^{jk2d(\cos\theta_{in}+\cos\theta_{out})}, \\ & \cdots, e^{jkd(\cos\theta_{in}+\cos\theta_{out})\cdot(M-1)}]^T \ .\end{aligned} \quad (6)$$

In URA configuration, assume there are M_x elements along the X-axis and M_y elements along the Y-axis, i.e., $M = M_x \cdot M_y$. In this case, both $\mathbf{\Omega}_{in}$ and $\mathbf{\Omega}_{out}$ contain azimuth angles and elevation angles that $\mathbf{\Omega}_{in} = (\psi_{in}, \theta_{in})$ and $\mathbf{\Omega}_{out} = (\psi_{out}, \theta_{out})$ that $\theta_{in}, \theta_{out} \in (0, \frac{\pi}{2})$ and $\psi_{in}, \psi_{out} \in (0, 2\pi)$. Finally, the steering vector $\boldsymbol{a}_C(\mathbf{\Omega}_{in}, \mathbf{\Omega}_{out})$ for URA could be expressed as

$$\begin{aligned}\boldsymbol{a}_C(\mathbf{\Omega}_{in}, \mathbf{\Omega}_{out}) =&[1, e^{j(\xi_x\cdot(1)+\xi_y\cdot(0))}, e^{j(\xi_x\cdot(2)+\xi_y\cdot(0))},\\ &e^{j(\xi_x\cdot(3)+\xi_y\cdot(0))}, \cdots, e^{j(\xi_x\cdot(m_x)+\xi_y\cdot(m_y))},\\ &\cdots, e^{j(\xi_x\cdot(M_x-1)+\xi_y\cdot(M_y-1))}]^T \ ,\end{aligned} \tag{7}$$

where $m_x \in (0, M_x - 1)$, $m_y \in (0, M_y - 1)$. In addition,

$$\xi_x = kd_x(\cos\psi_{in}\sin\theta_{in} + \cos\psi_{out}\sin\theta_{out}) \ , \tag{8}$$

$$\xi_y = kd_y(\sin\psi_{in}\sin\theta_{in} + \sin\psi_{out}\sin\theta_{out}) \ . \tag{9}$$

III. Half-Power Beamwidth

In this section, our focus is on IRS HPBW under natural reflection (i.e., $\boldsymbol{w} = 1$). However in the case of non-specular reflection, when the reflection angle is fixed, our derived analytical expressions and conclusions are still applicable with MRC beamforming.

A. HPBW of IRS in ULA Configuration

Because the transmission paths between elements are not equal, the phase shift of each element will also be different. Assume the total number of elements in ULA is M. According to (5), the AF of IRS could be defined as

$$AF = e^{j\xi_0} + e^{j\xi_1} + \cdots + e^{j\xi_m} + \cdots + e^{j\xi_{M-1}} \ , \tag{10}$$

where ξ_m are the merged phases of incident and reflection plane wave at the element locations $m = 1, 2, \cdots, M$ (referred to the physical center of the array). ϕ and α are the phase shifts between two elements in signal incident and reflection process, respectively. In this case,

$$\phi = kd\cos(\theta_{in}), \quad \alpha = kd\cos(\theta_{out}) \ . \tag{11}$$

We set $\xi = \phi + \alpha$. Since a large d (e.g., $d = \frac{2\lambda}{3}$) may lead to grating lobes causing interference and energy loss, a smaller d is preferred and the value of $\frac{\xi}{2}$ will be small, thus the equivalence of $sin(\frac{\xi}{2}) \approx \frac{\xi}{2}$ holds. According to (10) and (11), the AF could be normalized and then simplified to

$$AF = \frac{1}{M}\sum_{m=1}^{M} e^{j(m-1)(\phi+\alpha)} = \frac{1}{M}[\frac{\sin(\frac{M}{2}\xi)}{\sin(\frac{1}{2}\xi)}] \approx \frac{\sin(\frac{M}{2}\xi)}{\frac{M}{2}\xi}, \tag{12}$$

Since the normalized AF represents the amplitude of the beampattern, the 3-dB bandwidth point $\theta_{out,h}$ occurs when

$$20\cdot\lg(\frac{AF_h}{AF_{max}}) = -3 \ , \tag{13}$$

where AF_h is the magnitude of the beam pattern at 3-dB point and $AF_{max} = 1$ since AF is normalized. By solving (13) we obtain $AF_h = 0.707$. Thus, by referring to (11) and (12), the relationship between the incident angle θ_{in} and 3-dB bandwidth point $\theta_{out,h}$ is given by

$$\frac{\sin(\frac{M}{2}\xi)}{\frac{M}{2}\xi} = 0.707 \Rightarrow \frac{M}{2}kd(\cos\theta_{in} + \cos\theta_{out,h}) = \pm 1.391 \ . \tag{14}$$

There will be two solutions, $\theta_{out,h,1}$ and $\theta_{out,h,2}$ for (14), where $\theta_{out,h,1} = \cos^{-1}(\frac{2.782}{kMd} - \cos\theta_{in})$ and $\theta_{out,h,2} = \cos^{-1}(\frac{-2.782}{kMd} - \cos\theta_{in})$. Since $\theta_{out,max} = \pi - \theta_{in}$, the expression for Θ is

$$\Theta = \begin{cases} |\pi - \theta_{in} - \cos^{-1}(\frac{-2.782}{kMd} - \cos\theta_{in})| + \theta_{in} \ , \\ 0^\circ < \theta_{in} \le a \\ |\cos^{-1}(\frac{2.782}{kMd} - \cos\theta_{in}) - \cos^{-1}(\frac{-2.782}{kMd} - \cos\theta_{in})|, \\ a < \theta_{in} < b \\ |\pi - \theta_{in} - \cos^{-1}(\frac{2.782}{kMd} - \cos\theta_{in})| + \pi - \theta_{in} \ , \\ b \le \theta_{in} < 180^\circ \end{cases} \tag{15}$$

where a and b are the boundary values of whether the HPBW is affected by the bound of angle domain, and

$$a = \cos^{-1}(1 - \frac{2.782}{kMd}), \quad b = \cos^{-1}(\frac{2.782}{kMd} - 1) \ . \tag{16}$$

Physically, it means when the angle between the incident signal and IRS is smaller or greater than the boundary value a or b, respectively, not all the significant part (larger than 3dB) of the incident signal will be reflected to the position of Rx and can not be utilized easily or dissipate.

B. HPBW of IRS in URA Configuration

As shown in (5), AF will be the function of $\mathbf{\Omega}_{in}$ and $\mathbf{\Omega}_{out}$. That is, the function θ_{in}, θ_{out}, ψ_{in}, and ψ_{out}. According to (8) and (9), ξ_x and ξ_y represents the compound phase shifts at each elements on the IRS in X and Y axis, respectively. Assume there are M_x elements on X axis and M_y elements on Y axis, the expression of AF for a single element can be expressed as $AF = e^{j(m_x-1)\cdot\xi_x} \cdot e^{j(m_y-1)\cdot\xi_y}$, where $m_x = 1, 2, \cdots, M_x$ and $m_y = 1, 2, \cdots, M_y$. Thus, for the whole plane,

$$AF = \sum_{m_x=1}^{M_x} e^{j(m_x-1)\cdot\xi_x} \cdot \sum_{m_y=1}^{M_y} e^{jk(m_y-1)\cdot\xi_y} \ . \tag{17}$$

By simplification, the normalized AF could be expressed as

$$AF(\psi_{in}, \theta_{in}, \psi_{out}, \theta_{out}) = \{\frac{\sin(\frac{M_x}{2}\xi_x)}{\frac{M_x}{2}\xi_x}\}\{\frac{\sin(\frac{M_y}{2}\xi_y)}{\frac{M_y}{2}\xi_y}\} \ . \tag{18}$$

(17) and (18) are actually the results in ideal far-field case, while some works [9] have been proposed for deriving the IRS AF when considering pathloss. Here, it is important to obtain the location of the main lobe which is determined by $\theta_{out,max}$ and $\psi_{out,max}$. According to (18), there will be a main lobe only when $\xi_x = \xi_y = 0$ since the main lobe appears when the normalized AF reaches its maximum that $AF = AF_{max} = 1$. Thus, by referring to (8) and (9), the angles' relationships that allow $AF = 1$ are

$$\theta_{out,max} = \pi - \theta_{in} \ , \quad |\psi_{out,max} - \psi_{in}| = \pi \ . \tag{19}$$

In order to derive the HPBW from AF, there are two critical angles should be determined, $\theta_{out,h}$ and $\psi_{out,h}$, which represent the 3-dB bandwidth point. From (13), the angles' relationship that makes the main lobe reaches its half-power attenuation point could be expressed as

$$\{\frac{\sin(\frac{M_x}{2}\xi_x)}{\frac{M_x}{2}\xi_x}\}\{\frac{\sin(\frac{M_y}{2}\xi_y)}{\frac{M_y}{2}\xi_y}\} = 0.707 \ . \tag{20}$$

As shown in (20), there are four angles ψ_{in}, θ_{in}, ψ_{out} and θ_{out} that may affect AF, thus cause the different values of HPBW.

Based on the existing mathematical tools, it is hard to derive the expressions of HPBW directly in terms of these four variables. Therefore, we apply the method that represents the HPBW separately on azimuth and elevation plane since the two planes are orthogonal and independent to each other. Consider the incident and reflection angles on a certain plane as an angle set. Thus, there will be two sets of such angles' relations $(\theta_{in}, \theta_{out})$ and (ψ_{in}, ψ_{out}). Since the change of elevation angles is the main factor that causes the change in HPBW, we focus on the HPBW on the elevation plane. In this case, the expression of HPBW on elevation plane determined by $(\theta_{in}, \theta_{out})$ can be derived when the plane wave is reflected specular on azimuth plane with fixed ψ_{in}.

According to (8), (9) and (20), $\theta_{out,h}$ could be determined only if ψ_{in}, θ_{in} are fixed and $\psi_{out} = \psi_{out,max}$. Applying (19) that $|\psi_{out,max} - \psi_{in}| = \pi$, since (20) is a transcendental equation, $\theta_{out,h}$ could be expressed as an implicit function that

$$\theta_{out,h} = f(\theta_{in}, \psi_{in}) \ , \tag{21}$$

where $f(\theta_{in}, \psi_{in})$ is the solution of (20). Apparently, there will be a 3-dB bandwidth point on each side of the main lobe and we denote them as $\theta_{out,h,1}$ and $\theta_{out,h,2}$. Thus, the HPBW on elevation plane Θ_e could be expressed as

$$\Theta_e = |\theta_{out,h,1} - \theta_{out,h,2}| \ . \tag{22}$$

Θ_e has a closed form expression for some certain ψ_{in}. Here, we give the derivation for Θ_e when $\psi_{in} = 90°$ (in this case, $\psi_{out,max} = 270°$ according to (19)). According to (8), (9) and (20), we obtain the angle relationship that

$$\frac{\sin(\frac{M_y}{2}\xi_y)}{\frac{M_y}{2}\xi_y} = 0.707 \Rightarrow \frac{M_y}{2} k d_y (\sin\theta_{in} - \sin\theta_{out,h}) = \pm 1.391. \tag{23}$$

By solving (23), the 3-dB bandwidth points of Θ_e could be expressed as

$$\theta_{out,h} = \sin^{-1}(\sin\theta_{in} \pm \frac{2.782}{kM_y d_y}) \ . \tag{24}$$

Thus, Θ_e at $\psi_{in} = 90°$ could be expressed as

$$\Theta_e = \begin{cases} |\sin^{-1}(\sin\theta_{in} + \frac{2.782}{kM_y d_y}) - \sin^{-1}(\sin\theta_{in} - \frac{2.782}{kM_y d_y})|, \\ 0 < \theta_{in} \le c \ , \\ \\ \frac{\pi}{2} - \sin^{-1}(\sin\theta_{in} - \frac{2.782}{kM_y d_y}), \ c < \theta_{in} < \frac{\pi}{2} \ , \end{cases} \tag{25}$$

where $\theta_{in} \in (0, \frac{\pi}{2})$ since the range of elevation angles of the specular reflection does not involve the back of the IRS (the IRS is usually attached to the surfaces of physical objects). In addition, c is the boundary value for URA, and

$$c = \sin^{-1}(1 - \frac{2.782}{kM_y d_y}) \ . \tag{26}$$

IV. Simulation Results

In this part, we verify the analytical results (A.R.) of IRS HPBW conform to simulation results (S.R.) and make a comparison between the HPBW of the IRS and traditional active antenna array. As a benchmark, the HPBW of traditionally active antenna array [10] defined as Θ_t is expressed as

$$\Theta_t = |\frac{\pi}{2} - \cos^{-1}(\frac{2.782}{kMd})| + |\frac{\pi}{2} - \cos^{-1}(\frac{-2.782}{kMd})| \ . \tag{27}$$

The resolution of IRS to the signal determines the step size $\triangle\Omega$ between two inputs (incident angles) in simulation. From the definition of resolvability [13], the IRS can not resolve the signal from two directions when

$$\triangle\Omega = |\mathbf{\Omega}_{in,1} - \mathbf{\Omega}_{in,2}| \ll \frac{1}{L_r} \ , \tag{28}$$

where L_r is the normalized length of IRS. Hence, we set the step size $\triangle\Omega = 10^{-3} L_r^{-1}$ where $L_r = M \cdot d$ for the verification of HPBW on IRS in ULA configuration and $L_r = M_y \cdot d_y$ for HPBW on elevation plane in URA case.

A. Verification for HPBW on IRS in ULA configuration

In ULA case, we first verify (15) and then make a comparison between Θ and Θ_t. Set $d = \frac{\lambda}{2}$ and $M = 32, 64$, respectively. As shown in Fig. 1 where $M = 64$, the

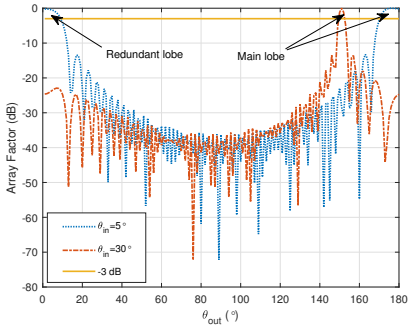

Fig. 1: Normalized AF of ULA IRS at different θ_{in}

main lobe of the IRS beampattern is truncated by the 3-dB bandwidth line, producing exactly two intersections, $\theta_{out,h,1}$ and $\theta_{out,h,2}$ when $\theta_{in} = 30°$. It is worth noting that the redundant lobe cannot be directly regarded as grating lobe defined in active antenna array since IRS and active array are essentially different. Here, since $\theta_{in} = 5°$ is less than the boundary value a determined by (16), part of the reflected signal energy will dissipate.

We then prove that the analytical expressions of Θ in (15) conform to S.R.. As shown in Fig. 2, Θ increases as θ_{in} moves away from 90° and reaches the maximum at $\theta_{in} = a, b$ determined by (16). As the incident signal gets closer to the surface of IRS, the more it will be dissipated, resulting in a decrease in Θ. Besides, Θ and Θ_t decrease simultaneously while M increases, which indicates that the greater the number of elements, the better the directivity of both systems will be. Although the two systems are different, their models are equivalent at vertical incidence, which explains why the two systems' HPBWs are equal at $\theta_{in} = 90°$ while the Θ is greater than Θ_t in the other incident conditions. We can also find that when the reflect/transmit angles are the same, the antenna array's HPBW $\Theta_{t,MRC}$ with MRC applied will be equal to Θ. Besides, unlike the HPBW of traditional active antenna array which is the overall response to the incident signals with different incident angles, the HPBW of IRS will change with incident angles. Also, larger d causes smaller HPBW and vice versa, which can be validated from formulas (15) and (25).

B. Verification for HPBW of IRS in URA configuration

In URA case, we first verify (25) and then make a comparison between Θ_e and Θ_t. Set $M_x = 8$, $d_y = \frac{\lambda}{2}$ and $M_y = 8, 32, 64$, respectively. Due to the symmetry of the

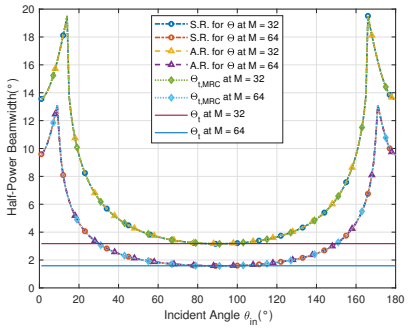

Fig. 2: Verification for HPBW of IRS in ULA configuration

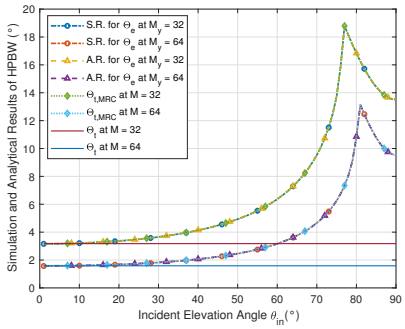

Fig. 4: Verification for HPBW of IRS in URA configuration

front and back of the IRS, we only consider the case where the signal is incident from the front, thus $\theta_{out} \in (0, \frac{\pi}{2})$ since the vertical incidence occurs when $\theta_{in} = 0°$. As shown in Fig. 3 where $M_x = M_y = 8$, when $\theta_{in} = 40°$, the main lobe intersects the 3-dB line, resulting in two intersections $\theta''_{out,h,1}$ and $\theta''_{out,h,2}$, thus $\Theta_e = |\theta''_{out,h,1} - \theta''_{out,h,2}|$. However, since the reflected signal energy will be dissipated more as the incident signal gets closer to the surface of IRS, $\theta_{out,h,1}$, which is greater than the boundary value c and closer to $90°$ than $\theta'_{out,h,1}$, leads to a narrower HPBW.

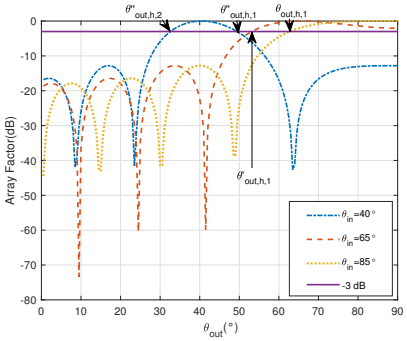

Fig. 3: Normalized AF of URA IRS at $\psi_{in} = 90°$

We then prove the analytical expressions of Θ_e in (25) conform to S.R.. Since Θ_e is the IRS HPBW on the elevation plane, which is the function of elevation angles for one-dimensional deployment since both ψ_{in} and ψ_{out} are constants, hence Θ_t can be used as a benchmark to measure the value of Θ_e. As shown in Fig. 4, Θ_e decreases while M_y increases, which indicate the better directivity of IRS will be obtained by increasing the number of elements. Similar to ULA case, except for the vertical incidence at $\theta_{in} = 0°$ where $\Theta_e = \Theta_t$, Θ_e is always greater than Θ_t. However, when the reflect/transmit angles are the same, the antenna array's HPBW $\Theta_{t,MRC}$ with MRC applied will be equal to Θ_e. As mentioned before, the boundary value c, which could be determined by (26), explains the abrupt changes in Θ_e.

V. Conclusions

Without considering channel path-loss and fading, this paper focuses on the expressions of IRS HPBW and discusses the HPBW difference between IRS and traditional active antenna array under the far-field condition. Based on the proposed system model, we derive the HPBW in both ULA and URA IRS configurations and prove the analytical expressions of the HPBW conform to the simulation results. We demonstrate the reason for the abrupt changes in the value of HPBW and prove the correctness of the analytical expressions for the boundary values. By comparing with the traditional active antenna array, we prove that the value of IRS HPBW will change with the incident angles when all weights are equal while generally, HPBW will change with reflect/transmit angle. In ULA and URA configurations, IRS HPBW is equal to antenna array's HPBW at the same reflect/transmit angle with MRC applied, while IRS HPBW is always greater than or equal to antenna array's HPBW when all weights are equal.

References

[1] G. L. Stuber, J. R. Barry, S. W. McLaughlin, Ye Li, M. A. Ingram, and T. G. Pratt, "Broadband MIMO-OFDM Wireless Communications," *Proceedings of the IEEE*, vol. 92, no. 2, pp. 271–294, 2004.

[2] S. V. Hum and J. Perruisseau-Carrier, "Reconfigurable Reflectarrays and Array Lenses for Dynamic Antenna Beam Control: A Review," *IEEE Transactions on Antennas and Propagation*, vol. 62, no. 1, pp. 183–198, 2013.

[3] N. I. Zheludev and Y. S. Kivshar, "From Metamaterials to Metadevices," *Nature materials*, vol. 11, no. 11, pp. 917–924, 2012.

[4] E. Basar, M. Di Renzo, J. De Rosny, M. Debbah, M.-S. Alouini, and R. Zhang, "Wireless Communications Through Reconfigurable Intelligent Surfaces," *IEEE Access*, vol. 7, pp. 116 753–116 773, 2019.

[5] T. S. Rappaport, S. Sun, R. Mayzus, H. Zhao, Y. Azar, K. Wang, G. N. Wong, J. K. Schulz, M. Samimi, and F. Gutierrez, "Millimeter Wave Mobile Communications for 5G Cellular: It Will Work!" *IEEE access*, vol. 1, pp. 335–349, 2013.

[6] Q. Wu and R. Zhang, "Intelligent Reflecting Surface Enhanced Wireless Network via Joint Active and Passive Beamforming," *IEEE Transactions on Wireless Communications*, vol. 18, no. 11, pp. 5394–5409, 2019.

[7] B. Zheng and R. Zhang, "Intelligent Reflecting Surface-Enhanced OFDM: Channel Estimation and Reflection Optimization," *IEEE Wireless Communications Letters*, vol. 9, no. 4, pp. 518–522, 2020.

[8] B. Zheng, C. You, and R. Zhang, "Intelligent reflecting surface assisted multi-user ofdma: Channel estimation and training design," *IEEE Transactions on Wireless Communications*, vol. 19, no. 12, pp. 8315–8329, 2020.

[9] W. Tang, M. Z. Chen, X. Chen, J. Y. Dai, Y. Han, M. Di Renzo, Y. Zeng, S. Jin, Q. Cheng, and T. J. Cui, "Wireless Communications with Reconfigurable Intelligent Surface: Path Loss Modeling and Experimental Measurement," *IEEE Transactions on Wireless Communications*, pp. 1–1, 2020.

[10] C. A. Balanis, *Antenna Theory: Analysis and Design*. John wiley & sons, 2016, pp. 285–351.

[11] Y. Liu, L. Zhang, B. Yang, W. Guo, and M. A. Imran, "Programmable Wireless Channel for Multi-user MIMO Transmission using Metasurface," in *2019 IEEE Global Communications Conference (GLOBECOM)*. IEEE, 2019, pp. 1–6.

[12] G. D. Durgin, *Space-Time Wireless Channels*. Prentice Hall Professional, 2003, pp. 233–240.

[13] D. Tse and P. Viswanath, *Fundamentals of Wireless Communication*. Cambridge university press, 2005, pp. 352–354.